Molecular Crystals and Liquid Crystals
Publication details, including instructions for authors and subscription information:
http://www.tandfonline.com/loi/gmcl20

Double Hydrogen Bonded Liquid Crystals Formed by Glutaric Acid

A. J. Gopunath [a], T. Chitravel [a], C. Kavitha [b], N. Pongali Sathya Prabu [b] & M. L. N. Madhu Mohan [b]

[a] Anna University Constituent College, Ramanathapuram, Tamil Nadu, India

[b] Liquid Crystal Research Laboratory (LCRL), Bannari Amman Institute of Technology, Sathyamangalam, Tamil Nadu, India

Published online: 02 Apr 2013.

To cite this article: A. J. Gopunath, T. Chitravel, C. Kavitha, N. Pongali Sathya Prabu & M. L. N. Madhu Mohan (2013) Double Hydrogen Bonded Liquid Crystals Formed by Glutaric Acid, Molecular Crystals and Liquid Crystals, 574:1, 19-32, DOI: 10.1080/15421406.2012.752306

To link to this article: http://dx.doi.org/10.1080/15421406.2012.752306

Mol. Cryst. Liq. Cryst., Vol. 574: pp. 19–32, 2013

ISSN: 1542-1406 print/1563-5287 online
DOI: 10.1080/15421406.2012.752306

Taylor & Francis
Taylor & Francis Group

Double Hydrogen Bonded Liquid Crystals Formed by Glutaric Acid

A. J. GOPUNATH,[1] T. CHITRAVEL,[1] C. KAVITHA,[2]
N. PONGALI SATHYA PRABU,[2]
AND M. L. N. MADHU MOHAN[2,*]

[1]Anna University Constituent College, Ramanathapuram, Tamil Nadu, India
[2]Liquid Crystal Research Laboratory (LCRL), Bannari Amman Institute of Technology, Sathyamangalam, Tamil Nadu, India

Homologous series of double hydrogen bonded liquid crystals are designed, synthesized, and characterized. Double hydrogen bond is formed between glutaric acid (GA) and p-n-alkyloxy benzoic acids (nBAO, where n varied from pentyl to dodecyl), resulting in new complexes referred as GA + nBAO. Formation of hydrogen bond is conformed by the Fourier transform infra red spectroscopy. The synthesized mesogens are characterized by polarizing optical microscopy, differential scanning calorimetric studies, ensuing phase diagram from the obtained data. The isolated mesogens are found to exhibit orthogonal and tilted phases, namely, nematic, smectic C, smectic F, and smectic G. In addition to these characteristic phases, a new smectic ordering labeled as smectic X has been identified and characterized. Dielectric studies are performed to confirm the newly formed smectic X phase. Thermal equilibrium and odd even effect are evinced from the individual enthalpy values of the homologues. The magnitudes of experimental optical tilt angle in smectic C of all the homologues is fitted to a power law, and the value of exponent is found to concur with the mean field theory predicted value.

Keywords Dielectric studies; hydrogen bonded liquid crystals; optical tilt angle; smectic X

1. Introduction

Design and synthesis of functional organo mesogenic materials with the aid of noncovalent interactions took a new turn in the scientific society for the past few decades [1–12]. Forming self-assembly systems by means of intermolecular hydrogen bonding, which exists between the chemical moieties, made the worldwide scientists to focus their interest on this intermolecular hydrogen bonding. Hydrogen bonding, the fifth type of fundamental force enables various mesogenic and nonmesogenic compounds to form complexes with rich liquid crystalline character [7]. Hydrogen bonding plays a crucial role in assembling the molecules through noncovalent interactions. Activation energy possessed by the molecules and the lower bonding exhibited by them influences the thermal properties such as clearing points, enthalpies, and mesomorphic phase behavior [10] of the formed mesogens. Stable

*Address correspondence to M. L. N. Madhu Mohan, Liquid Crystal Research Laboratory (LCRL), Bannari Amman Institute of Technology, Sathyamangalam 638401, Tamil Nadu, India. Tel.: +91-9442437480; Fax: +91-4295-223775. E-mail: mln.madhu@gmail.com

molecular complexes are prepared by simple, molecular self-assembly process, using such hydrogen bonding. A number of such hydrogen bonded liquid crystal (HBLC) systems have been reported by Kato and Frechet [13–15], which indicates that the mesomorphism results from proper combination of molecular interactions and shape of the molecules. It is also proved that this hydrogen bonding has pronounced influence on crystallization and phase behaviors of multicomponent supramolecular complexes formed by benzoic acids.

A few systems consisting of hydrogen bonds functioning between identical molecules were also known. Depending upon the length of the chain, type of bonding and the functional groups present in the HBLCs exhibit a rich variety of phase polymorphism and hence, the molecular structure of HBLC and the physical properties exhibited by them are correlated. The application aspects and commercial viabilities made many research groups to work on these HBLC systems [6–10].

The carboxylic acids with other acids are reported to form single, double, and even multiple hydrogen bonds. Through our previous experience [16–32] in designing, synthesizing, and characterizing various types of liquid crystals, a successful attempt has been made in characterizing a novel series of homologues formed from glutaric acid (GA) and p-n-alkyloxy benzoic acids (GA + *n*BAO, where *n* varied from pentyl to dodecyl) through inter molecular hydrogen bonding. In this communication, thermal and dielectric characterizations of the present homologous series are also discussed in detail.

2. Experimental

Optical textural observations were made with Nikon polarizing microscope equipped with Nikon digital charge-coupled device camera system with 5 mega pixels and 2560 × 1920 pixel resolutions. Liquid crystalline textures were stored, retrieved, and analyzed with the aid of ACT-2U imaging software system. Temperature control of the liquid crystal cell was equipped by Instec HCS402-STC 200 temperature controller (Instec, Boulder, CO) to a temperature resolution of $\pm 0.1^{\circ}$C. This unit was further interfaced to a computer by IEEE–STC 200 to control and monitor the temperature. Liquid crystal sample was filled by capillary action in its isotropic state into a commercially available (Instec, USA) polyamide buffed cell with 4-μm spacer. Optical extinction technique [33] was used for the determination of tilt angle. Transition temperatures and corresponding enthalpy values were experimentally deduced by differential scanning calorimetric (DSC) (Shimadzu DSC-60, Kyoto, Japan). Fourier transform infra red (FTIR) spectra was recorded (ABB FTIR MB3000, Quebec, Canada) and analyzed with the MB3000 software. Dielectric studies were performed with HP4192A LF impedance analyzer. The GA and *n*BAO were supplied by Sigma Aldrich (Munich, Germany), and all the solvents used were of high-performance liquid chromatography grade.

2.1. Synthesis of HBLC

The present intermolecular hydrogen bonded mesogens are obtained by the addition of two moles of *n*BAO with one mole of GA in N,N-dimethyl formamide (DMF) and reprecipitating after the evaporation as reported in literature [34–36]. The scheme of synthesis and the general molecular structure of the present homologous series of GA+nBAO are depicted in Fig. 1, where *n* represents the alkyloxy carbon number, which varies from pentyl to dodecyl.

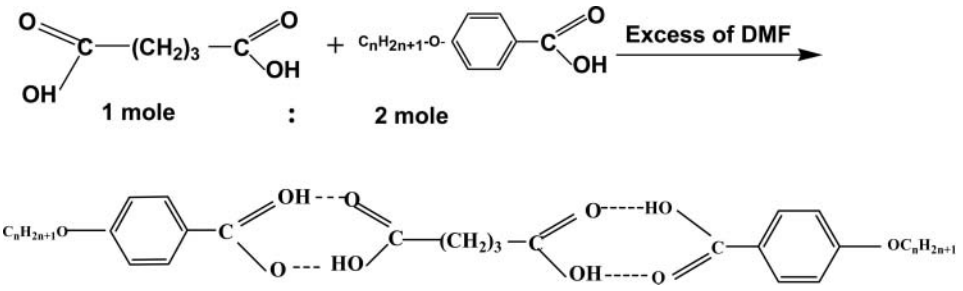

Figure 1. Synthesis scheme representing the formation of GA + *n*BAO hydrogen bonded series and the molecular structure of GA + *n*BAO homologous series.

3. Results and Discussion

The HBLCs isolated in the present study are white crystalline solids and are stable at room temperature (∼30°C). They are insoluble in water and sparingly soluble in common organic solvents, such as methanol, ethanol, benzene, and dichloromethane. However, they show a high degree of solubility in coordinating solvents like dimethyl sulfoxide, DMF, and pyridine. All these mesogens melt at specific temperatures below approximately 98°C (Table 1). They show high thermal and chemical stability when subjected to repeated thermal scans performed during polarizing optical microscopy (POM) and DSC studies.

3.1. Phase Identification

The DSC data in the cooling and heating cycles for the entire GA + *n*BAO series are presented in Table 1 from which the phase variance, transition temperatures, and corresponding enthalpy values are clearly given. It is found that these data are in concurrence with POM data. The isolated mesogens are found to exhibit characteristic textures [37], namely, nematic (droplet texture, plate 1), smectic C (broken focal conic texture, plate 2),

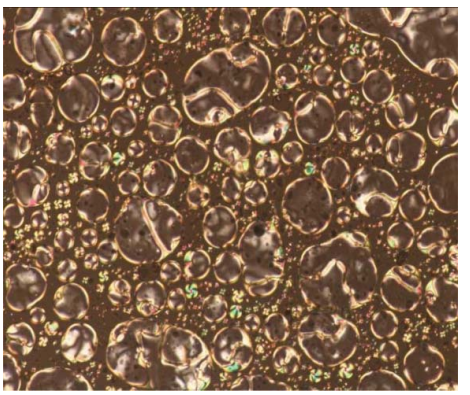

Plate 1. Nematic droplets of GA + 12BAO complex.

Table 1. Transition temperatures and enthalpy values obtained by various techniques of GA + *n*BAO homologous series

Complex	Phase variance	Study	Crystal to melt	N	X	C	F	G	Crystal
GA + 5BAO	G	DSC (h)	91.9 (42.91)					@	
		DSC (c)						102.2(78.66)	70.1 (47.95)
		POM (c)						102.9	70.6
GA + 6BAO	NG	DSC (h)	90.1 (31.42)	109.9(0.88)				@	
		DSC (c)		100.9 (1.64)				84.2 (36.58)	73.9(28.53)
		POM (c)		101.5				84.6	74.1
GA + 7BAO	NG	DSC (h)	89.8 (89.96)	@				@	
		DSC (c)		106.6 (0.75)				80.4 (29.47)	72.3 (50.80)
		POM (c)		107.1				80.7	72.5
GA + 8BAO	NCG	DSC (h)	73.2 (20.23)	@		@		94.7 (27.9)	
		DSC (c)		132.8 (0.43)		108.3 (0.38)		87.6 (16.34)	65.8 (7.99)
		POM (c)		133.4		108.8		87.9	66.0
GA + 9BAO	NCG	DSC (h)	93.7 (110.47)	@		@		@	
		DSC (c)		100.9 (1.26)		85.5 (28.25)		76.7 (#)	73.1 (79.82)
		POM (c)		101.6		86.1		77.1	73.3
GA + 10BAO	NCG	DSC (h)	95.3(39.16)	@		@		@	
		DSC (c)		100 (1.77)		90.1 (26.58)		74.2 (#)	71.7 (43.11)
		POM (c)		100.7		90.6		74.6	71.9
GA + 11BAO	NXCFG	DSC (h)	97.7(103.5)	@	@	@	@	@	
		DSC (c)		103.4 (0.68)	102.1 (0.85)	96.2 (1.56)	82.5(42.69)	70.4 (17.78)	47.9 (39.13)
		POM (c)		104.3	102.8	96.8	83.0	70.7	48.1
GA + 12BAO	NXCFG	DSC (h)	95.1(76.56)	@	@	@	@	@	
		DSC (c)		136.4 (0.09)	128.3 (0.46)	126	85.3(21.99)	70.3 (#)	67 (16.37)
		POM (c)		137.2	129.0	126.7	85.8	70.6	67.2

(c): cooling run, (h): heating run, #: not resolved, @: monotropic transition. Temperatures in degrees centigrade, enthalpy values (J/g) given in parenthesis.

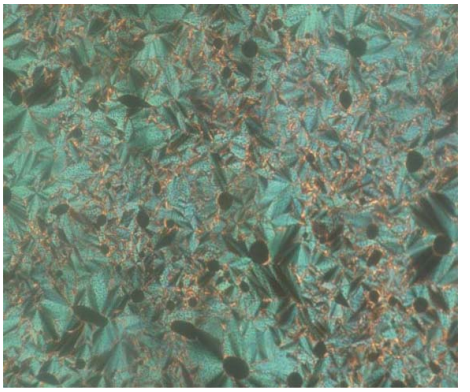

Plate 2. Broken focal conic texture of smectic C in GA + 12BAO complex.

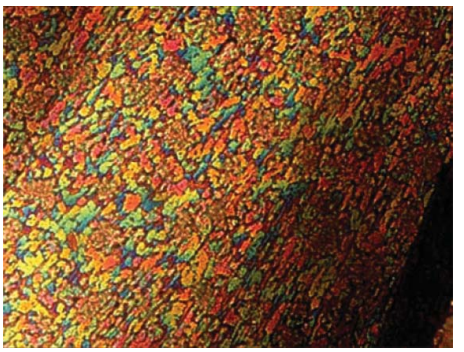

Plate 3. Chequered board texture of smectic F in GA + 12BAO complex.

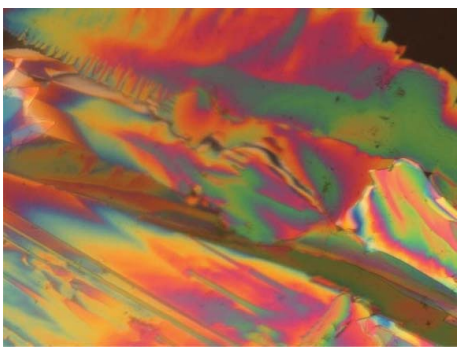

Plate 4. Multicolored mosaic texture smectic G in GA + 12BAO complex.

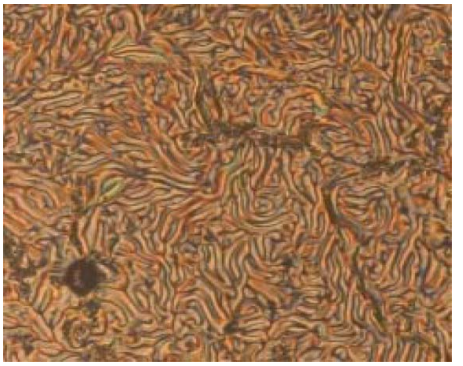

Plate 5. Fully grown smectic X phase observed in GA + 12BAO complex.

smectic F (chequered board texture, plate 3), and smectic G (multicolored mosaic texture, plate 4). In addition to these characteristic phases, a new smectic ordering designated as smectic X (worm like texture, plate 5) has also been identified in this series. A close look at plate 1 indicates point singularities with four brushes and are characterized by $s = 1$. In smectic C, the change of color of the broken focal conic texture with temperature is inferred to the changes in birefringence of the material. When the smectic G phase (plate 4) is formed on cooling smectic F, it constitutes of mosaic platelets, which are quite large and are highly colored.

General phase sequence of the various GA + *n*BAO homologues in the cooling and heating run of POM and DSC can be shown as

$$\text{Isotropic} \rightarrow \text{Sm G} \rightleftharpoons \text{Crystal} \quad (\text{GA} + 5\text{BAO})$$

$$\text{Isotropic} \rightarrow \text{N} \rightarrow \text{Sm G} \rightleftharpoons \text{Crystal} \quad (\text{GA} + 6\text{BAO}, \text{GA} + 7\text{BAO})$$

$$\text{Isotropic} \rightarrow \text{N} \rightleftharpoons \text{Sm C} \rightleftharpoons \text{Sm G} \rightleftharpoons \text{Crystal} \quad (\text{GA} + 8\text{BAO}, \text{GA} + 9\text{BAO}, \text{GA} + 10\text{BAO})$$

$$\text{Isotropic} \rightarrow \text{N} \rightarrow \text{Sm X} \rightarrow \text{Sm C} \rightarrow \text{Sm F} \rightarrow \text{Sm G} \rightleftharpoons \text{Crystal} \quad (\text{GA} + 11\text{BAO}, \text{GA} + 12\text{BAO})$$

Monotropic and enantiotropic transitions are depicted as single and double arrows, respectively.

3.2. Fourier Transform Infrared Spectroscopy

The FTIR spectra of *n*BAO, GA, and their intermolecular hydrogen bonded complex are recorded in the solid state (KBr) at room temperature. As a representative case, FTIR spectrum of GA + 11BAO is shown in Fig. 2. The solid state spectra of pure *n*BAO is reported [38,39] to have two sharp bands at 1685 cm^{-1} and 1695 cm^{-1} due to the ν (C=O) stretching mode. The doubling feature of this stretching mode confirms the dimeric nature of the complex at room temperature [39]. Furthermore, a strong intense band appearing at 2920 cm^{-1} is assigned to ν (O−H) carboxylic acid group. On the whole, these evidences act in favor of hydrogen bond formation in the present homologues.

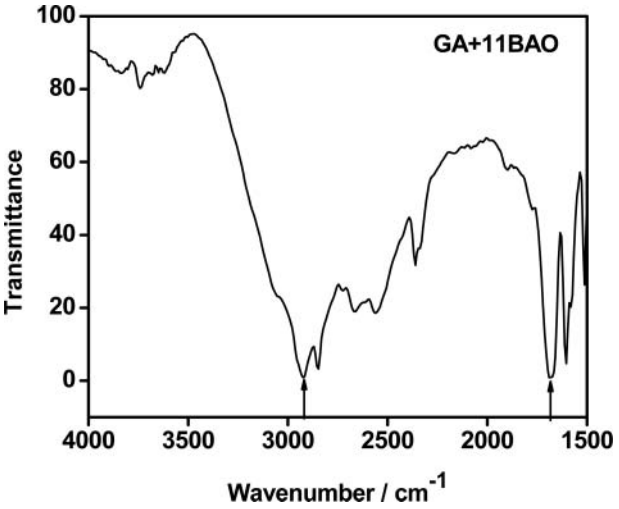

Figure 2. FTIR spectra of GA + 11BAO complex.

3.3. DSC Studies

The DSC thermograms are recorded in heating and cooling cycle. The empty aluminium pan is weighed initially, and the accurately weighed mesogen is filled in it before crimping. The crimped aluminium pan along with the sample is placed in the heating chamber of DSC. Another crimped empty aluminium pan is taken as the reference. In the heating chamber, nitrogen gas is flushed out at a constant rate. DSC thermograms are recorded, stored, and analyzed by TA60 data software. The mesogen is heated with a predetermined scan rate of 10°C min^{-1} and held at its isotropic temperature for 2 minutes so as to attain thermal stability. The exothermic run is performed with an identical scan rate of 10°C min^{-1}, and the DSC thermogram of GA + 7BAO is illustrated in Fig. 3 as a representative case.

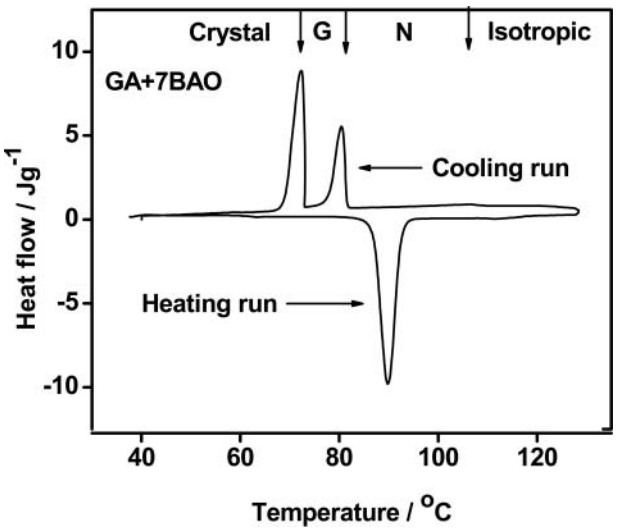

Figure 3. DSC thermogram of GA + 7BAO complex.

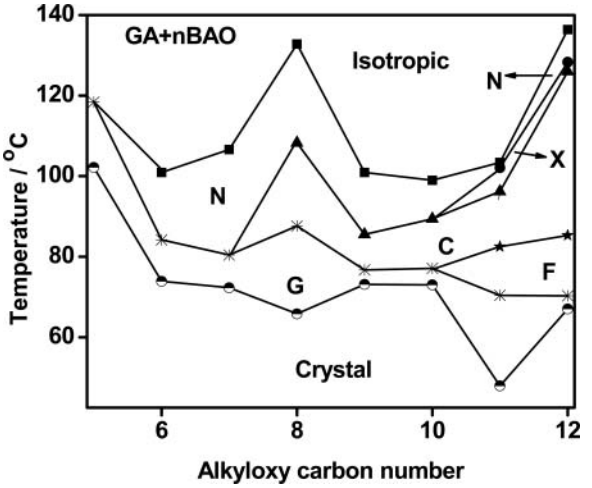

Figure 4. Phase diagram of GA + *n*BAO homologous series.

Experimentally obtained equilibrium transition temperatures and corresponding enthalpy values of the mesogens are listed separately in Table 1. It can be noticed that POM studies reasonably concur with the DSC transition temperatures.

3.4. Phase Diagram of GA+ n*BAO Series*

The phase diagram of the present homologous series (GA + *n*BAO) is constructed through the data obtained from POM studies and DSC data. The phase diagram of pure *n*BAO is reported [20] to exhibit two phases, namely, nematic and smectic C. Phase diagram of GA + *n*BAO homologous series is depicted in Fig. 4. Following points can be elucidated from Fig. 4:

(1) GA + *n*BAO homologous series exhibits nematic as orthogonal phase and smectic C, smectic X, smectic G, and smectic F as tilted phases.
(2) Nematic phase is observed in all the homologous series with the exception of GA + 5BAO.
(3) A systematic inducement of the phases occurs with respect to the linear increment in the carbon chain length of the homologous series.
(4) The increase of *l*/*d* ratio with chain length of the series favors the inducement of various phases.
(5) Smectic C is induced only in the higher homologues starting from octyloxy benzoic acid and prevails throughout the series.
(6) Higher order smectic G phase is seen throughout the series, whereas smectic F is found only in the two higher homologues.
(7) Compared to the precursors, three smectic phases, namely, smectic X, smectic F, and smectic G are induced in the present homologous series.
(8) Smectic X phase is induced only in undecyloxy benzoic acid and dodecyloxy benzoic acid, quenching the thermal range of smectic C. Further smectic X is sandwiched between nematic and smectic C phases.

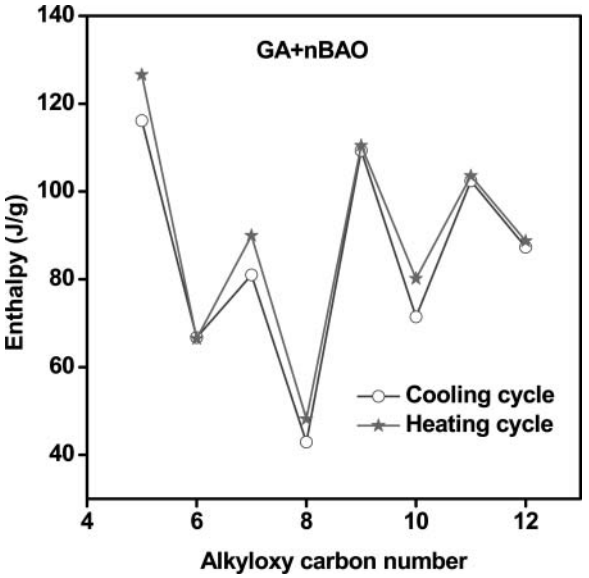

Figure 5. Odd–even effect with respect to summation of enthalpy values of various phase transitions in GA + *n*BAO homologous series.

The *l*/*d* ratio of the homologous series is attributed to the occurrence of smectic X phase. The absence of smectic X phase in the lower homologues reflects the absence of threshold value of *l*/*d* ratio.

3.5. Thermal Equilibrium and Odd–Even Effect

The DSC thermograms in cooling and heating cycle of all the members of GA + *n*BAO homologous series are recorded at a scan rate of 10°C min^{-1} and tabulated in Table 1. From Table 1, the sum of enthalpies corresponding to various phase transitions of individual homologues (GA + *n*BAO) in heating cycle and cooling cycle are computed. Figure 5 is constructed with alkyloxy number on X-axis and the corresponding sum of enthalpy values on Y-axis. It is interesting to note from Fig. 5 the following points.

(1) The sum of enthalpies in heating cycle is marginally higher than the sum of enthalpies in cooling cycle for all the homologues in GA + *n*BAO series. Thus in Fig. 5, the heating and cooling lines follow one another closely. This indicates that the total amount of heat energy evolved in exothermic process is equal to the total amount of heat absorbed in endothermic process of the complexes in the entire GA + *n*BAO series. This result is a token of evidence for possessing thermal equilibrium with respect to heat flow.

(2) Furthermore, the even complexes, namely, GA + 6BAO, GA + 8BAO, GA + 10BAO, and GA + 12BAO follow a pattern of results while their counterparts, i.e., the odd complexes, namely, GA + 3BAO, GA + 7BAO, GA + 9BAO, and GA + 11BAO follow another pattern of results. In the literature [40,41], this is referred as odd–even effect. It can also be noticed that the odd complexes posses higher value of enthalpies compared to their successive even complexes.

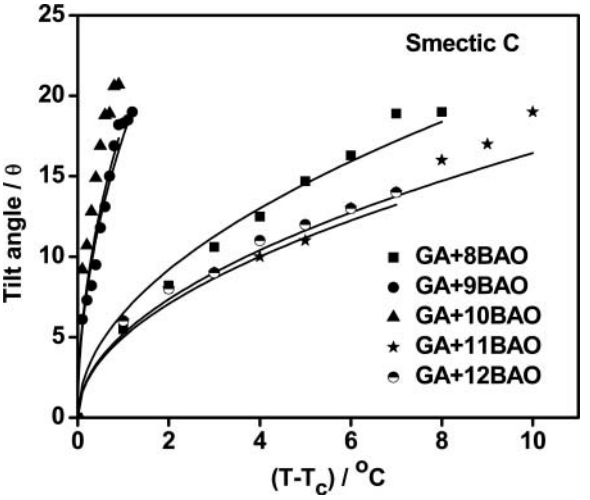

Plate 6. Optical tilt angle measurement in smectic C phase of GA + *n*BAO complexes.

4. Smectic C and Measurement of Optical Tilt Angle

Smectic C phase has been identified as the tilted phase, where the molecular long axes of the constituent molecules are tilted with respect to normal to the layer planes. The occurrence of smectic C phase and its dependence on the molecular structure and temperature has been thoroughly verified by numerous experimental studies. The conclusions and the findings from these results suit best for the present series (GA + *n*BAO) under investigation, and they can be concluded as

(1) Smectic C phase is very well dependent upon the molecular structure of the constituent molecules, that too on the length of the carbon chain and the alkyloxy terminal groups.
(2) Smectic C phase existing in this series depends on the structures having two terminal groups, namely, alkyloxy groups attached to the rigid core of benzene.
(3) Symmetrical molecular structures (benzoic acids) also favor the growth of smectic C phase in the homologous series.

As the smectic C phase depends upon the temperature, the optical tilt angle has been experimentally measured by optical extinction method in smectic C phase of all the members of the present homologous series (GA + *n*BAO). Figure 6 depicts such variation of optical tilt angle with temperature for GA + *n*BAO (where $n = 8$ to 12) series. In Fig. 6, the theoretical fit obtained is denoted by the solid line. Furthermore, the tilt angle increases with decreasing temperature. For the complex GA + 10BAO, the magnitude of tilt angle is observed to be around $\sim 20^\circ$. These larger magnitudes of the tilt angle are attributed to the direction of the soft covalent hydrogen bond interaction which spreads along molecular long axis with finite inclination. Tilt angle is a primary order parameter [42], and the temperature variation is estimated by fitting the observed data of $\theta\ (T)$ to the relation,

$$\theta\,(T)\,\alpha\,(T_C - T)^{\beta} \tag{1}$$

The critical exponent β value estimated by fitting the data of $\theta\ (T)$ to the above equation (1) is found to be 0.50 to agree with the mean field prediction [43,44]. Furthermore, the

agreement of magnitude of β (0.5) with mean field predicted value (0.5) infers the long-range interaction of transverse dipole moment for the stabilization of tilted smectic C phase.

5. Characterization of Smectic X Phase

On slow cooling from nematic phase at a rate of 0.1°C min^{-1}, a new phase labeled as smectic X is observed. The darker part of the worm and its opposite handed is clearly visualized in plate 5, which determines the phase to be tilted. This phase stabilizes as the temperature is further decreased, and the corresponding fully grown smectic X phase texture is shown in plate 5. The worms are curved and are observed throughout the liquid crystal cell. In fact, they act as the grating elements, which manifest the helicoidal structure of this phase. The observation of first- and second-order diffraction pattern in this phase is a token of evidence for the presence of helicoidal structure. In the entire thermal span of this phase, neither the size (diameter) nor the length of the worms is altered. On further decrement of temperature, broken focal conic texture of smectic C (plate 2) is observed. These results are in concurrence with our previously reported data [29,31,32].

6. Dielectric Studies

A second-order transition, which goes unobserved in the DSC study, can very well be detected with dielectric studies. GA + 12BAO complex of the present homologous series is considered as a representative case for this study, and the variation of capacitance and dielectric loss with temperature is performed in this present investigation. A commercially available 4-μm polyamide buffed cell (Instec, Boulder, CO, USA) with an active area of 1 mm^2 is filled with the mesogen (GA + 12BAO) by capillary action. Silver wires are drawn from the cell as lead contact. The empty liquid crystal cell is calibrated with temperature and a known substance (benzene) to calculate the leads capacitance. The cell filled with mesogen is placed in an Instec Hot and Cold Stage (HCS 402), whose temperature is monitored by an Instec stand-alone temperature controller unit (STC 200), interfaced to the computer, to an accuracy of ±0.1°C. The sample is taken to its clearing point and hold for 2 minutes so as to attain thermal stability. Simultaneous textural observations are also made to ascertain the phase of the mesogen and are corelated with the dielectric data. The readings are noted in the cooling run with a scan rate of 0.1°C. GA + 12BAO complex filled in the liquid crystal cell is provided with a sinusoidal stimulus of 1.1 V obtained from HP4192A impedance analyzer. The variation of the capacitance for the frequencies 10 kHz and 100 kHz is plotted in Fig. 7, in which all the phase transition temperatures are observed. As a result, the dielectric spectrum and the textural transition temperatures are studied together. The dielectric spectrum of GA + 12BAO complex is depicted in Fig. 7 for further clarification. From Fig. 7, the following points can be inferred.

(1) A small knick is observed at 135.3°C, as the temperature is decreased from isotropic state, indicating the onset of the nematic phase. A droplet texture was observed with the onset of nematic phase.
(2) At 128°C, the magnitude of permittivity encounter a sudden decrement, indicating the onset of smectic X followed immediately by smectic C. Furthermore, a worm like texture instantly followed by a broken focal conic smectic C texture in textural analysis proves this.

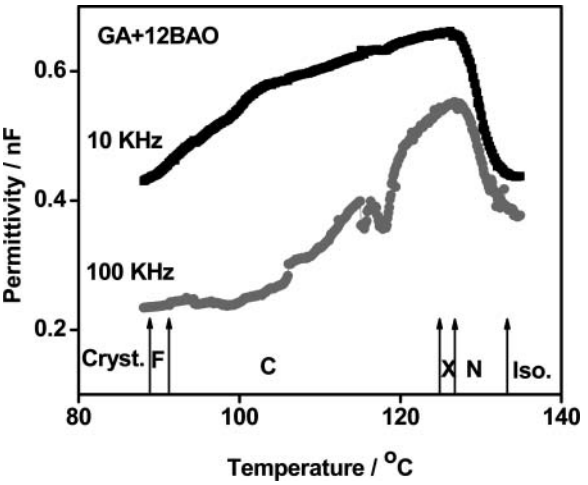

Plate 7. Permittivity variance with temperature of GA + 12BAO complex at 10 kHz and 100 kHz.

(3) The permittivity started decreasing without any sudden anomaly in the dielectric spectrum after 128°C, indicating the stabilization of the smectic C phase.
(4) A chequered board texture of smectic F phase acts as an evidence for the occurrence of smectic F phase, where the curve slightly shows an irregularity at nearly 86°C.
(5) As the succeeding phase, smectic G phase is found merged with the crystal, it is not clearly visualized in the figure.

The transition temperatures obtained by this technique is in fine agreement with POM and DSC studies.

7. Conclusions

(1) A novel series of HBLC is synthesized and characterized by various techniques.
(2) A new smectic ordering, namely, smectic X phase has been observed in certain complexes.
(3) Phase diagram is drawn from the textural observation and DSC studies.
(4) Odd–even effect is discussed in the enthalpy values of the entire homologous series.
(5) Optical tilt angle for all the complexes in the smectic C phase is measured and fitted to power law.

Acknowledgments

Graceful blessings of Almighty Bannari Amman and the infrastructural support rendered by Bannari Amman Institute of Technology are gratefully acknowledged. The authors (MLNMM, CK, NPS) would like to thank the financial support rendered by BRNS - DAE, India, vide sanction number 2012/34/35/BRNS/1033.

References

[1] Paleos, C. M., & Tsiourvas, D. (1995). *Angew.Chem. Intl. Ed. Engl.*, *34*, 1696. Paleos, C. M., & Tsiourvas, D. (2001). *Liq.Cryst.*, *28*, 1127.
[2] Sideratou, Z., Tsiourvas, D., Paleos, C. M., & Skoulios, A. (1997). *Liq. Cryst.*, *22*, 51.
[3] Fukumasa, M., Kato, T., Uryu, T., & Frechet, J. M. J. (1993). *Chem. Lett.*, 65.
[4] Malik, S., Dhal, P. K., & Mashelkar, R. A. (1995). *Macromolecules*, *28*, 2159.
[5] Kihara, H., Kato, T., Uryu, T., & Frechet, J. M. J. (1996). *Chem. Mater.*, *8*, 961.
[6] Petrov, M. P., & Tsonev, L. V. (1996). *Liq.Cryst.*, *21*, 543.
[7] Xu, B., & Swager, T. (1996). *J. Chem. Soc.*, *117*, 5011.
[8] Clark, N. A., & Lagerwall, S. T. (1980). *Appl. Phys. Lett.*, *36*, 899.
[9] Fukuda, A., & Takezoe, H. (1990). *Structures and Properties of Liquid Crystals*, Corona: Tokyo, Japan.
[10] Kumar, P. A., Srinivasulu, M., & Pisipati, V. G. K. M. (1999). *Liq. Cryst.*, *26*, 1939.
[11] Kato, T., Fujishima, A., & Frechet, J. M. J. (1990). *Chem. Lett.*, 919.
[12] Yu, L. J. (1993). *Liq.Cryst.*, *14*, 1303.
[13] Kato, T., & Frechet, J. M. J. (1995). *Macromol. Symp.*, *95*, 311.
[14] Kato, T., & Frechet, J. M. J. (1989). *J. Am. Chem. Soc.*, *111*, 8533.
[15] Kato, T., & Frechet, J. M. J. (1989). *Macromolecules*, *22*, 3818.
[16] Pongali Sathya Prabu, N., Vijayakumar, V. N., & Madhu Mohan, M. L. N. (2011). *Mol. Cryst. Liq. Cryst*., *548*, 73.
[17] Vijayakumar, V. N., & Madhu Mohan, M. L. N. (2009). *Braz. J. Phy.*, *39*(4), 677.
[18] Pongali Sathya Prabu, N., Vijayakumar, V. N., & Madhu Mohan, M. L. N. (2011). *J. Mol. Str*., *994*, 387.
[19] Pongali Sathya Prabu, N., Vijayakumar, V. N., & Madhu Mohan, M. L. N. (2011). *Physica B*., *406*, 1106.
[20] Pongali Sathya Prabu, N., Vijayakumar, V. N., & Madhu Mohan, M. L. N. (2012). *Phase Transitions*, *85*, 149.
[21] Pongali Sathya Prabu, & Madhu Mohan, M. L. N. (2012). *Phase Transitions*, *85*, 592.
[22] Vijayakumar, V. N., Murgugadass, K., & Madhu Mohan, M. L. N. (2010). *Mol. Cryst. Liq. Cryst.*, *517*, 43.
[23] Chitravel, T., & Madhu Mohan, M. L. N. (2010). *Mol. Cryst. Liq. Cryst.*, *524*, 131.
[24] Vijayakumar, V. N., & Madhu Mohan, M. L. N. (2010). *Mol. Cryst. Liq. Cryst.*, *517*, 113.
[25] Vijayakumar, V. N., & Madhu Mohan, M. L. N. (2009). *J. Opto. Elec. Adv. Mat.*, *11*(8), 1139.
[26] Vijayakumar, V. N., & Madhu Mohan, M. L. N. (2009). *Sol. State. Sci.*, *4*, 482.
[27] Vijayakumar, V. N., & Madhu Mohan, M. L. N. (2009). *Sol. State. Comm.*, *149*, 2090.
[28] Pongali Sathya Prabu, N., Vijayakumar, V. N., & Madhu Mohan, M. L. N. (2011). *Mol. Cryst. Liq. Cryst*., *548*, 142.
[29] Kavitha, C., & Madhu Mohan, M. L. N. (2012). *JPCS*, *73*, 1203.
[30] Pongali Sathya Prabu, N., Potukuchi, D. M., & Madhu Mohan, M. L. N. (2012). *Physica B*, *407*, 3709.
[31] Kavitha, C., Pongali Sathya Prabu, N., & Madhu Mohan, M. L. N. (2012). *Physica B*, *407*, 859.
[32] Pongali Sathya Prabu, N., Vijayakumar, V. N., & Madhu Mohan, M. L. N. (2012). *Mol. Cryst. Liq. Cryst*., *557*, 190.
[33] Noot, C., Perkins, S. P., & Coles, H. J. (2000). *Ferroelectrics*, *244*, 331.
[34] Kihara, T., Kato, T., Ujiie, S., Uryu, T., Kumar, U., Frechet, J. M. J., Bruce, D. W., & Price, D. J. (1996). *Liq. Cryst.*, *21*, 25.
[35] Kato, T., Kihara, T., Ujiie, S., Uryu, T., & Frechet, J. M. J. (1996). *Macromolecules*, *29*, 8734.
[36] Kato, T., Uryu, T., Kaneuchi, F., Jin, C., & Frechet, J. M. J. (1993). *Liq. Cryst.*, *14*, 1311.
[37] Gray, G. W., & Goodby, J. W. G. (1984). *Smectic Liquid Crystals: Textures and Structures*, Leonard Hill: London, U.K.
[38] Pavia, D. L., Lampman, G. M., & Kriz, G. S. (2007). *Introduction to Spectroscopy*, Sanat Printers: Kundli, Haryana, India.

[39] Nakamoto, K. (1978). *Infrared and Raman Spectra of Inorganic and Co-ordination Compounds*, Interscience: New York.
[40] Marcelja, S. (1974). *J. Chem. Phys.*, *60*, 3599.
[41] Chandrasekhar, S. (1977). *Liquid Crystals*, Cambridge University Press: New York.
[42] De Gennes, P. G. (1974). *The Physics of Liquid Crystals*, Oxford Press: London, U.K.
[43] Barmatov, E. B., Bobrovsky, A., Barmatova, M. V., & Shibaev, V. P. (1999). *Liq. Cryst.*, *26*, 581.
[44] Stanley, H. E. (1971). *Introduction to Phase Transition and Critical Phenomena*, Clarendon Press: New York.